Martensitic fcc-to-hcp Transformations in Solid Xenon under Pressure: A First-Principles Study

Eunja Kim* and Malcolm Nicol

Department of Physics and High Pressure Science and Engineering Center, University of Nevada, Las Vegas, Nevada 89154, USA

Hyunchae Cynn and Choong-Shik Yoo

H-Division, Physics and Advanced Technology Directorate, Lawrence Livermore National Laboratory, University of California, Livermore, California 94550, USA

(Received 7 October 2005; published 24 January 2006)

First-principles calculations reveal that the fcc-to-hcp pressure-induced transformation in solid xenon proceeds through two mechanisms between 5 and 70 GPa. The dynamics of the phase transition involves a sluggish stacking-disorder growth at lower pressures (path I) that changes to a path involving an orthorhombic distortion at higher pressures (path II). The switchover is governed by a delicate interplay of energetics (enthalpy of the system for the structural stability) and kinetics (energy barrier for the transition). The two types of martensitic transformations involved in this pressure-induced structural transformation are a twinned martensitic transition at lower pressures and a slipped martensitic transition at higher pressures.

DOI: 10.1103/PhysRevLett.96.035504 PACS numbers: 61.50.Ks, 61.50.Ah, 64.70.Kb, 71.15.Nc

Martensitic transformations have been observed in many interesting materials such as metals, ceramics, proteins, and shape-memory alloys [1–4]. These transitions are characterized by a collective movement of atoms and very often are accompanied by microstructures such as twinning and slipping [5]. Solid xenon has a face-centered-cubic (fcc) crystal structure at low temperature and ambient pressure. It transforms into the hexagonal-close-packed (hcp) structure under pressure [6–10]. Recent angle-resolved x-ray diffraction patterns of Xe revealed that a martensitic fcc-to-hcp transformation takes place between 3 and 70 GPa in diamond-anvil cells. The transformation is very sluggish but persists until completion [8]. The evolution of the angle-resolved x-ray diffraction data suggests that the two phases coexist over a wide pressure range. These observations are surprising because the thermodynamic condition for coexistence of two phases of the same substance is that the Gibbs free energies of both phases are the same, and it is unlikely that such an equality persists over a wide range of pressures at a particular temperature [11]. Over decades, a large number of experimental [6–9] and theoretical studies [12–18] have been devoted to understanding the mechanism or sequence of pressure-induced phase transformations in solid xenon. However, a quantitative study that explains what causes this transformation to be very sluggish and yet very persistent is still missing.

Several scenarios have been proposed to explain the changes in the x-ray diffraction patterns occurring during the pressure-induced fcc-to-hcp transformation in solid xenon. One interpretation is that an unknown intermediate phase intervenes between these pressures [7]; another is that the fcc and hcp phases coexist [8,17]. The present work has two aims: to provide a quantitative understanding of phase transformation mechanisms under pressure and to shed light on the origin of the sluggishness during the transformation and on the underlying mechanism for the persistence in completing this transformation. A phenomenological description of the phase transformation in solid xenon may be a generic example of situations encountered in the pressure-induced structural transformations of element solids such as Kr [9], Co [19], and Pb [20].

The similar energies and structures of the fcc and the hcp phases are challenges for accurately describing solid xenon. However, density-functional theory (DFT) with the local-density approximation (LDA) has been successfully applied to studying rare-gas solids under pressure [16,17,21] since the van der Waals contribution becomes less important with increasing pressure [22–24]. For total-energy calculations, we use the first-principles FHI98MD code [25,26]. This is a fully self-consistent DFT method which employs standard norm-conserving pseudopotentials. We used the LDA by Ceperley and Alder [27] as parametrized by Perdew and Zunger [28] and tested both Hamann [29] and Troullier-Martins [30] types of norm-conserving pseudopotentials. Results presented in this Letter are obtained by using Hamann-type pseudopotentials since they produced slightly better structural parameters compared to experiments. The kinetic energy was cut off at 70 Ry. Large supercells were used, up to 32 atoms for enthalpy calculations and 48 atoms to calculate energy barriers. The k-point integration is performed with mesh points corresponding to 8 $\mathbf{k}$ points in the Brillouin zone. The total energy was minimized by using the damped Joannopoulos algorithm [31].

Our calculated structural properties for the fcc phase such as the equilibrium volume, 38.08 cm^3/mol, and bulk modulus, 3.81 GPa, are in excellent agreement with recent experimental data, 37.97 cm^3/mol and 3.6 GPa, respectively [8]. Such agreement suggests that this ap-

proach provides a solid theoretical framework for modeling the structural evolution and transformation of Xe at high pressure. The difference between the calculated and experimental fcc lattice constants becomes negligible at higher pressures. For example, the calculated lattice constant of the fcc phase at 25 GPa, 4.85 Å, is in excellent agreement with the experimental value, 4.86 Å. Our density-functional calculations also predict a difference of only 0.02 eV in cohesive energy between the fcc and hcp phases at ambient conditions. Details will be discussed elsewhere [32]. The energy barriers for the stacking-disorder growth pathway (path I) and an alternative pathway involving an intermediate orthorhombic distortion (path II) were examined using DFT calculations to understand the underlying transformation mechanisms. For path I, the fcc stacking grows into hcp domains, as previously proposed [8], through sliding of adjacent {111} planes. This changes the stacking order along the ⟨111⟩ direction from the $ABCABC\cdots$ to the $ABABAB\cdots$. In this scheme a large supercell with 48 atoms in six layers was used to simulate the twinned martensitic [5] fcc-to-hcp transformation in solid xenon. If the first and second layers are fixed, sliding the third and fourth layers relative to the first two layers switches the stacking order from $ABCABC\cdots$ to $ABABCA\cdots$. At the same time, the fifth and sixth layers slide relative to the third and fourth layers, changing in the stacking order from $ABABCA\cdots$ to $ABABAB\cdots$.

Figure 1 shows the calculated energy barriers for path I at several pressures. At ambient pressure, the very small energy barrier, 0.02 eV/atom, facilitates the fcc-to-hcp stacking growth. However, the barrier increases with pressure and becomes fairly large, 0.26 eV/atom, at 25 GPa. This large barrier explains the sluggishness of the fcc-to-hcp transformation observed in experiments [8] since the majority of xenon is still in the fcc phase which is stable at low pressures. Our DFT calculations confirm, below 25 GPa, the recently proposed fcc stacking-disorder growth mechanism for the transformation [8]. At lower pressures, stacking disorder in the fcc lattice grows into hcp domains as pressure increases because the hcp structure becomes more stable and the energy costs of stacking faults are very small. Despite the sluggishness of this structural transformation and the increasing activation energy barrier, it takes place persistently up to 70 GPa. This suggests that the underlying mechanism changes at higher pressures, but to what? At pressures above 25 GPa, enthalpy calculations of Xe indicate that the fcc stacking becomes unstable to an orthorhombic distortion. This instability leads to an alternative transformation pathway leading to the hcp phase (path II).

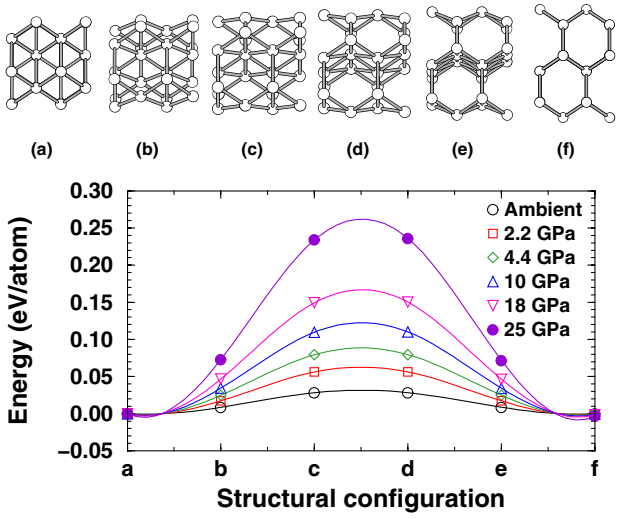

FIG. 1 (color online). The calculated energy barrier for the stacking disordered growth (path I) transformation pathway at 0, 2.2, 4.4, 10, 18, and 25 GPa. The energy is calculated relative to the value of the fcc phase at the same pressure. The initial configuration (a) is the fcc phase, and the final configuration (f) is the hcp phase. In the structural representations, the [111] direction of the fcc phase is coming out of the page.

Path II through the orthorhombic distortion was simulated by enthalpy calculations. Figure 2 shows results for fcc, hcp, and face-centered orthorhombic (fco) Xe. These results imply that the transformation from the fcc to the hcp phase starts at about 5 GPa, in good agreement with experiments [7,8] and previous theoretical calculations [16,17]. The enthalpies of fco and hcp Xe stay very close to the enthalpy of fcc Xe, about 70 GPa. Above 70 GPa, the enthalpies of the fco and hcp phases differ dramatically from the enthalpy of the fcc phase. These differences are consistent with experiments which show that the fcc-to-hcp transformation is complete around 70 GPa. The fact that enthalpies of the fcc and fco phases cross at 22 GPa is consistent with the experimental observation of the sudden jump in the intensity of the hcp phase around 25 GPa. Our results suggest that this sudden jump is due to the appearance of the orthorhombic distortion, which makes solid Xe overcome the increasing sluggishness of the fcc-to-hcp sliding mechanism because of the larger energy barrier at higher pressures as shown in Fig. 1. That is, at 25 GPa, the

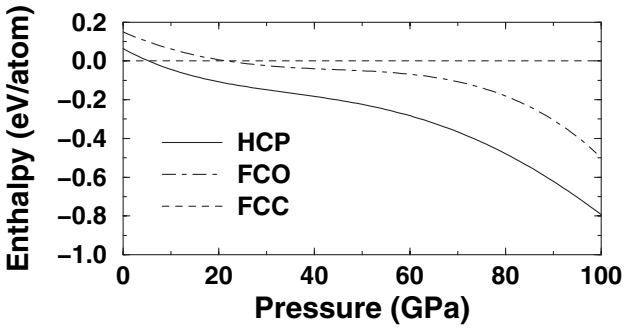

FIG. 2. The calculated enthalpies of the fcc, hcp, and fco phases of solid xenon. The fcc phase is the reference. The solid line and dot-dashed line indicate the hcp and fco phases, respectively.

orthorhombic distortion provides an energetically more favorable pathway for the transformation from the fcc phase (path II).

In modeling path II, the orthorhombic structure was considered as the intermediate in the fcc-to-hcp transformation. Although group theoretical analysis [33] based on the symmetries of the initial fcc and final hcp structures allow either a monoclinic or orthorhombic intermediate, comparison of our simulated x-ray diffraction patterns with recent experimental diffraction data [8] suggests that the face-centered orthorhombic structure (fco, $F222$ space group) is the only possible intermediate. Details of these structures of Xe will be discussed elsewhere [32].

Figure 3 shows the calculated energy change along path II at 25 GPa where the orthorhombic structure has lower enthalpy than the cubic phase as shown in Fig. 2. A different plane sliding scheme is applied for path II. The {001} planes are divided into two groups with each adjacent plane belonging to different groups. The transition involves one group moving relative to the other along the ⟨010⟩ direction to complete the slipped martensitic fco-to-hcp transformation [5]. Since the {111} planes slide most easily for the fcc structure, the {001} sliding scheme is energetically unfavorable in the fcc phase. However, the stability of the orthorhombic distortion makes this possible. This is explained by the larger interlayer distance and, therefore, weaker interatomic interactions between adjacent {001} planes in the fco structure.

Once the orthorhombic distortion begins, there is no energy barrier to impede further transformation to the hcp phase along ⟨010⟩ as shown in Fig. 3. This explains why path II becomes dominant at higher pressures where the energy barrier for path I continues to increase. These results present a clear picture of the pressure-induced structural transformation in xenon. Path I, the stacking-disorder growth in {111} planes, is the main transformation mode at pressures below 25 GPa; then path II, involving the orthorhombic distortion followed by spontaneous atomic rearrangements to the pure hcp phase, takes over at higher pressures. These results also explain why a fco phase of Xe has not been identified experimentally.

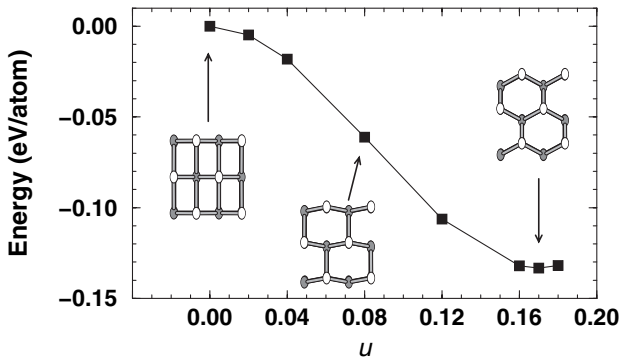

FIG. 3. The calculated energies for path II at 25 GPa and 0 K. The parameter u represents the relative shear of adjacent planes along the [010] direction and is normalized by the lattice constant b. The fco (hcp) structure corresponds to $u = 0$ (1/6). Energy is calculated relative to the fco phase. The [001] direction is perpendicular to the page, and the [010] direction is upward. Atoms represented by open circles move in the [010] direction relative to those represented by filled circles.

Figure 4 shows the calculated volume compressions for fcc, hcp, and fco Xe, which agree closely with the experimental data [8]. There is an excellent agreement between theory and experiment for the fcc phase at $P < 25$ GPa and for the hcp phase at $P > 68$ GPa. In the pressure range of 25 to 68 GPa, the experimental data nominally assigned to the fcc phase lie between the theoretical results for fcc and hcp phases as shown in Fig. 4(a). However, the calculated volume compression results for the fco phase lie on top of the experimental data as shown in Fig. 4(b), which is remarkable since the calculations involved no adjustable parameters. These results provide a distinct quantitative description of the fcc and hcp phases of Xe and clearly suggest that the fco structure is an intermediate in the fcc-to-hcp transformation in Xe. Although the orthorhombic structure satisfies the necessary conditions imposed by group theory for an intermediate, an appropriate simulated x-ray diffraction pattern, and computed equation of states between 25 and 68 GPa, the calculations also prove that it is not an intermediate phase but only a transitory state along the reaction path. Indeed, the system transits through this structure to overcome the energy barrier of path I.

In summary, we have demonstrated that the fcc-to-hcp transformation in solid xenon proceeds via two mechanisms. At pressures below 25 GPa, the transition proceeds via a stacking-disorder growth mechanism (path I). At higher pressures, the mechanism changes to follow a dis-

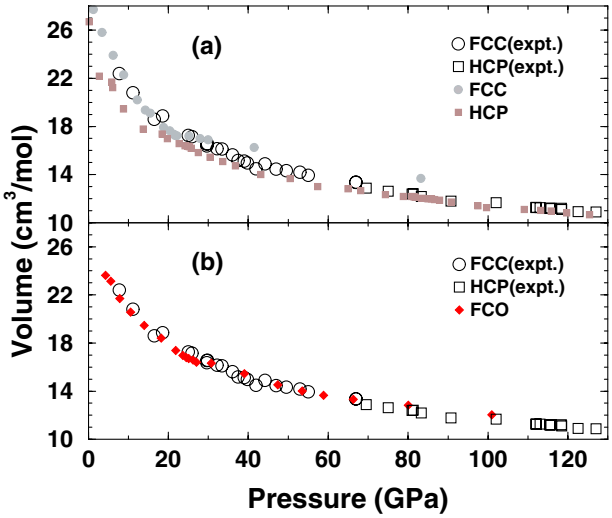

FIG. 4 (color online). Calculated volume compressions for (a) fcc and hcp phases, and (b) fco phase. Open circles and squares represent experimental data for the fcc and hcp phases, respectively [8]. Filled circles, squares, and diamonds represent theoretical data for the fcc, hcp, and fco phases.

tortion through a structure with fco symmetry (path II). The assignment of the fco structure is based on symmetry constraints as well as structural and enthalpy calculations which closely agree with experiment. The measured sudden change in x-ray intensity at around 25 GPa is identified as the signature of the mechanistic switch. The calculated energy barrier results provide a quantitative explanation for the sluggishness of the fcc-to-hcp transformation and highlight the mechanism for switching to path II at high pressure. These results resolve the long-standing issue of the mechanism for the pressure-induced structural transformation in Xe. A systematic study on similar phenomena observed in other materials such as Ar and Kr will provide a better understanding of the delicate interplay between energetics and kinetics during the structural transformation.

We acknowledge valuable discussions with C. Chen at the University of Nevada, Las Vegas. We also thank D. M. Hatch at Brigham Young University on group-theory based symmetry constraints and M. Parrinello and G. Tabacchi of ETH-Zurich for the xenon pseudopotentials. This work was supported in part by the Department of Energy (DOE) Cooperative Agreement FC08-01NV14049 with the University of Nevada, Las Vegas. The work at Lawrence Livermore National Laboratory (LLNL) has been performed under the auspices of the U.S. DOE by the University of California under Contract No. W-7405-Eng-48. We are grateful to the San Diego Supercomputer Center for support in computing resources.

*Electronic address: kimej@physics.unlv.edu

[1] G. B. Olsen and W. Owen, *Martensite* (ASM International, Materials Park, OH, 1992).
[2] E. K. H. Salje, *Phase Transitions in Ferroelastic and Coelastic Crystals* (Cambridge University Press, Cambridge, 1993).
[3] V. C. Solomon, M. R. McCartney, and D. J. Smith, Y. Tang, A. E. Berkowitz, and R. C. O'Handley, Appl. Phys. Lett. **86**, 192503 (2005).
[4] K. Bhattacharya, S. Conti, G. Zanzotto, and J. Zimmer, Nature (London) **428**, 55 (2004).
[5] K. Kadau, T. C. Germann, P. S. Lomdahl, and B. L. Holian, Science **296**, 1681 (2002).
[6] M. Ross and A. K. McMahan, Phys. Rev. B **21**, 1658 (1980).
[7] A. P. Jephcoat, H. K. Mao, L. W. Finger, D. E. Cox, R. J. Hemley, and C. S. Zha, Phys. Rev. Lett. **59**, 2670 (1987).
[8] H. Cynn, C. S. Yoo, B. Baer, V. Iota-Herbei, A. K. McMahan, M. Nicol, and S. Charlson, Phys. Rev. Lett. **86**, 4552 (2001).
[9] D. Errandonea, Beate Schwager, Reinhard Boehler, and Marvin Ross, Phys. Rev. B **65**, 214110 (2002).
[10] R. Boehler, M. Ross, P. Söderlind, and D. B. Boercker, Phys. Rev. Lett. **86**, 5731 (2001).
[11] The Gibbs phase rule states that the degree of freedom is defined as $F = C + 2 - P$ for a system with C components in P phases, which limits the degree of freedom in the thermodynamic system. For example, solid Xe has 1 degree of freedom, since $C = 1$ for one component and $P = 2$ for the two phases to remain in equilibrium.
[12] C. P. Herrero and R. Ramirez, Phys. Rev. B **71**, 174111 (2005).
[13] R. Reichlin, K. E. Brister, A. K. McMahan, M. Ross, S. Martin, Y. K. Vohra, and A. L. Ruoff, Phys. Rev. Lett. **62**, 669 (1989).
[14] H. Chacham, X. Zhu, and S. G. Louie, Phys. Rev. B **46**, 6688 (1992).
[15] A. B. Belonoshko, R. Ahuja, and B. Johansson, Phys. Rev. Lett. **87**, 165505 (2001).
[16] J. K. Dewhurst, R. Ahuja, S. Li, and B. Johansson, Phys. Rev. Lett. **88**, 075504 (2002).
[17] W. A. Caldwell, J. H. Nguyen, B. G. Pfrommer, F. Mauri, S. G. Louie, and R. Jeanloz, Science **277**, 930 (1997).
[18] F. Saija and S. Prestipino, Phys. Rev. B **72**, 024113 (2005).
[19] C. S. Yoo, H. Cynn, P. Soderlind, and V. Iota, Phys. Rev. Lett. **84**, 4132 (2000).
[20] V. P. Dmitriev and S. B. Rochal, Phys. Rev. Lett. **62**, 2495 (1989).
[21] T. Tsuchiya and K. Kawamura, J. Chem. Phys. **117**, 5859 (2002).
[22] T. Iitaka and T. Ebisuzaki, Phys. Rev. B **65**, 012103 (2002).
[23] I. Kwon, L. A. Collins, J. D. Kress, and N. Troullier, Phys. Rev. B **52**, 15 165 (1995).
[24] M. Springborg, J. Phys. Condens. Matter **12**, 9869 (2000).
[25] M. Bockstedte, A. Kley, J. Neugenbaur, and M. Scheffler, Comput. Phys. Commun. **107**, 187 (1997).
[26] M. Fuchs and M. Scheffler, Comput. Phys. Commun. **119**, 67 (1999).
[27] D. M. Ceperley and B. J. Alder, Phys. Rev. Lett. **45**, 566 (1980).
[28] J. P. Perdew and A. Zunger, Phys. Rev. B **46**, 6671 (1992).
[29] D. R. Hamann, Phys. Rev. B **40**, 2980 (1989).
[30] N. Troullier and J. L. Martins, Phys. Rev. B **43**, 1993 (1991).
[31] M. C. Payne, M. P. Teter, D. C. Allan, T. A. Arias, and J. D. Joannopoulos, Rev. Mod. Phys. **64**, 1045 (1992).
[32] E. Kim, M. Nicol, H. Cynn, and C. S. Yoo (unpublished).
[33] H. T. Stokes and D. M. Hatch, Phys. Rev. B **65**, 144114 (2002).